

University of Wollongong

## Research Online

---

Faculty of Engineering and Information  
Sciences - Papers: Part A

Faculty of Engineering and Information  
Sciences

---

1-1-2013

### Condition monitoring of slow speed slewing bearing based on largest lyapunov exponent algorithm and circular-domain feature extractions

Wahyu Caesarendra

*University of Wollongong, wc026@uowmail.edu.au*

Prabuono Buyung Kosasih

*University of Wollongong, buyung@uow.edu.au*

A Kiet Tieu

*University of Wollongong, ktieu@uow.edu.au*

Craig A. S Moodie

*University of Wollongong, cam920@uow.edu.au*

Follow this and additional works at: <https://ro.uow.edu.au/eispapers>



Part of the [Engineering Commons](#), and the [Science and Technology Studies Commons](#)

---

#### Recommended Citation

Caesarendra, Wahyu; Kosasih, Prabuono Buyung; Tieu, A Kiet; and Moodie, Craig A. S, "Condition monitoring of slow speed slewing bearing based on largest lyapunov exponent algorithm and circular-domain feature extractions" (2013). *Faculty of Engineering and Information Sciences - Papers: Part A*. 2273.

<https://ro.uow.edu.au/eispapers/2273>

Research Online is the open access institutional repository for the University of Wollongong. For further information contact the UOW Library: [research-pubs@uow.edu.au](mailto:research-pubs@uow.edu.au)

---

# Condition monitoring of slow speed slewing bearing based on largest Lyapunov exponent algorithm and circular-domain feature extractions

## Abstract

This paper presents a combined nonlinear and circular features extraction-based condition monitoring method for low speed slewing bearing. The proposed method employs the largest Lyapunov exponent (LLE) algorithm as a signal processing method based on vibration data. LLE is used to detect chaos existence in vibration data in discrete angular positions of the shaft. From the processed data, circular features such as mean, skewness and kurtosis are calculated and monitored. It is shown that the onset and the progressively deteriorating bearing condition can be detected more clearly in circular-domain features compared to time-domain features. The application of the method is demonstrated with laboratory run slewing bearing data.

## Keywords

feature, domain, circular, exponent, Lyapunov, extractions, largest, condition, bearing, slewing, speed, slow, monitoring, algorithm

## Disciplines

Engineering | Science and Technology Studies

## Publication Details

Caesarendra, W., Kosasih, B., Tieu, A. Kiet. & Moodie, C. A. S. (2013). Condition monitoring of slow speed slewing bearing based on largest Lyapunov exponent algorithm and circular-domain feature extractions. 26th International Condition Monitoring and Diagnostic Engineering Management Congress (COMADEM) United Kingdom: Condition Monitoring and Diagnostic Engineering Management.

# Condition Monitoring of Low Speed Slewing Bearing based on Largest Lyapunov Exponent Algorithm and Circular-Domain Feature Extractions

Wahyu Caesarendra<sup>1\*</sup>, Buyung Kosasih<sup>1</sup>, Anh Kiet Tieu<sup>1</sup>, Craig A.S. Moodie<sup>1</sup>

<sup>1</sup>School of Mechanical, Materials and Mechatronics Engineering, University of Wollongong, Wollongong, NSW 2522, Australia,

\*e-mail: wc026@uowmail.edu.au

Keywords: condition monitoring, low speed slewing bearing, largest Lyapunov exponent, circular-domain feature extraction

## Abstract

This paper presents a combined nonlinear and circular features extraction-based condition monitoring method for low speed slewing bearing. The proposed method employs the largest Lyapunov exponent (LLE) algorithm as a signal processing method based on vibration data. LLE is used to detect chaos existence in vibration data in discrete angular positions of the shaft. From the processed data, circular features such as mean, skewness and kurtosis are calculated and monitored. It is shown that the onset and the progressively deteriorating bearing condition can be detected more clearly in circular-domain features compared to time-domain features. The application of the method is demonstrated with laboratory run slewing bearing data.

## Nomenclature

---

BPFI	Ball Pass Frequency of Inner Race
BPFO	Ball Pass Frequency of Outer Race
BSF	Ball Spin Frequency
$J$	Lag time or reconstruction delay
$k$	Circular kurtosis
$M$	Numbers of vectors reconstructed
$m$	Embedding dimension
$N$	Number of data points of vibration signal
$s$	Circular skewness
$r$	Radius of two dimensional plane
$R$	Resultant vector length
$\mathbf{X}$	Phase space or reconstruction vectors
$\mathbf{x}$	Time series vibration data, $\mathbf{x} = (x_1, x_2, \dots, x_N)$
$Z_i$	Two-dimensional plane of $\alpha_i$
$\bar{Z}$	Circular mean
$\alpha$	Negative $\lambda_1$ sign in circular domain, $\alpha = (\alpha_1, \alpha_2, \dots, \alpha_i)$
$\beta$	Reversible angle of slewing bearing
$\Delta t$	Sampling period of vibration signal
$\lambda_1$	Largest Lyapunov exponent

---

## 1. Introduction

Slewing bearing is the rolling element bearing commonly used in large industrial machineries such as turntables, steel mill cranes, offshore cranes, rotatable trolleys, excavators, reclaimers, stackers, swing shovels and ladle cars. They typically support high axial and radial loads. Slewing bearings are often critical production parts. An unplanned downtime when one of these bearings breaks down can be very costly due to the interruption of production. Moreover, as replacement of large slewing bearings takes long lead time to arrive due to long manufacturing and delivery time, plants often carry spare bearings to guard against these unforeseen circumstances, adding extra cost. In order to prevent extended unplanned downtimes, an accurate condition monitoring method is needed.

The accuracy of the condition monitoring method depends on the selection of the monitored features. The change in rolling element bearing condition is usually reflected by changes in the vibration signal features. However, it is difficult to select the proper features for the slow speed slewing bearing case ( $\approx 1$  rpm). Statistical time-domain features which are commonly used in high speed rolling element bearings show low sensitivities when applied to low rotational speed slewing bearings due to the low impact energy emission as the rotating elements contact with defect spots (Tan, et al 2008). The low energy impact generates a very weak vibration signal which is deeply masked by the background noise. Because the features are taken from the vibration signal where the noise is dominant, they are insensitive to any alteration in the bearing condition. When eventually the vibration amplitude exceeds the background noise, the features values do increase significantly but at this point

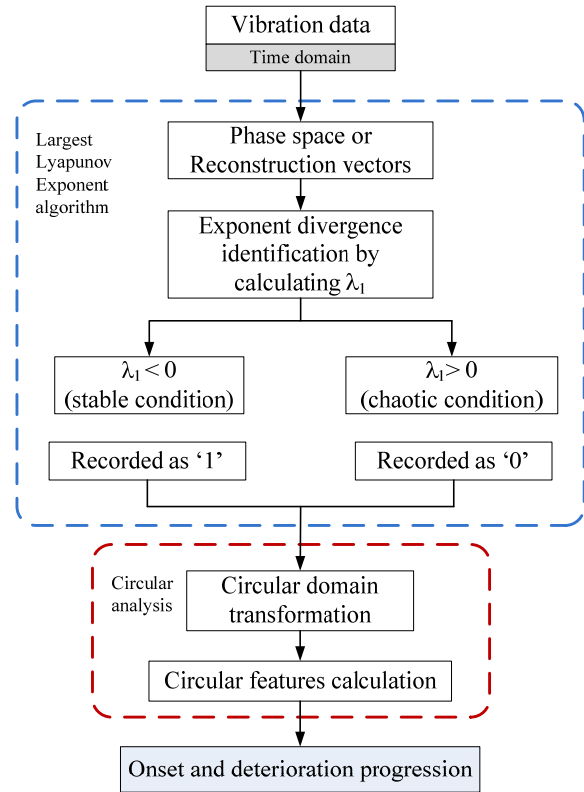
serious bearing damages have already occurred: often by this stage the bearing condition is already close to unsustainable fault.

Most published articles in slewing bearing research employed finite element method analysis (Kania, 2006; Göncz, et al 2011; Gang, et al 2011; Glodež, et al 2012; Aguirrebeitia, et al 2012). There are few which use oil analysis (Bai, et al 2011; Liu, 2007), and even fewer which discuss vibration monitoring techniques (Rodger, 1979). (Žvokelj, et al 2010) and (Žvokelj, et al 2011) presented a vibration analysis techniques based on ensemble empirical mode decomposition (EEMD) combined with multi-scale principal component analysis (MSPCA). The method was successfully used to monitor data from a lab slewing bearing where a fault was induced by an artificial single defect. In practice, due to low speeds, high load conditions and reversible rotations, the fault in slewing bearing is considered as due to multiple defects. Therefore, a signal processing technique to identify the occurrence of multiple defects is necessary.

With large diameter slewing bearings, multiple defects can be identified by using a special data processing method which assesses the bearing condition in discrete angular positions of the shaft. In this paper, the combination of largest Lyapunov exponent (LLE) as a data processing method and circular features calculation as the monitored variables is employed. LLE is a common method to identify chaotic behaviour of time series, whereas circular features are used to statistically analyse the behaviour of distributed data in an angular or circular domain. LLE is usually used in medical engineering (Päivinen, et al 2005) and circular features are commonly used in the biological and neuroscience fields [Berens, 2009; Fisher, 1995; Pewsey, 2004]. Neither method has been used in the vibration condition monitoring (CM) area to date. The two fsteps of the proposed method are illustrated in Picture 1. In step 1, the time series vibration data is reconstructed with predetermined embedding dimension and lag time, and the stable and chaotic condition in vibration signal based on reconstructed vectors is identified using LLE algorithm every 1 s ( $\approx 6^\circ$ ). Using the reconstructed vectors as the input, the LLE algorithm measures the exponential divergence,  $\lambda_1$  of the reconstructed vector. Further, the vibration condition is determined from the sign of  $\lambda_1$ . If the sign is negative, i.e.  $\lambda_1 < 0$ , it will imply stable condition, while  $\lambda_1 > 0$  implies chaos condition. Stable condition occurrence is recorded as '1' and chaos condition is recorded as '0'. By transforming the position of condition '1' in the angular domain, circular features such as

mean, skewness and kurtosis can be computed in step 2 of the proposed method.

The proposed method is demonstrated with laboratory run slewing bearing data. The results show the superior effectiveness of the proposed method in monitoring the condition of slow speed slewing bearing from normal to failure, compared to time-domain features extraction.



Picture 1 General steps of the proposed combined largest Lyapunov exponent and circular-domain feature extraction method

## 2. Largest Lyapunov Exponent (LLE) Algorithm

When a fault occurs in a slewing bearing, the dynamical contact between rolling elements and defect spots will produce a local instability vibration signal. Due to the low rotational speed, the impact energy is relatively low and short and, thus, the local instability signal is deeply masked in background noise. Using the conventional time-domain features such as mean, root mean square, skewness and kurtosis the degradation progress from normal to faulty condition is difficult to identify. In order to overcome the drawback, a combined LLE algorithm, as a signal processing, and circular features as a monitored variable are used. Among the potential nonlinear features such

as fractal dimension, correlation dimension and LLE, the last one is selected in this paper due to its capability in identifying chaotic conditions by positive or negative signs (Päivinen, et al 2005). This characteristic is useful for the circular analysis method, as shown later.

In order to analyse nonlinear and chaotic characteristics, the original time series vibration signal,  $\mathbf{x} = (x_1, x_2, \dots, x_N)$  is reconstructed, where  $N$  is the number of data points of the vibration signal. In common terms, the reconstructed vectors are said to form a phase space. The phase space can be defined as follows:

$$\mathbf{X} = \begin{bmatrix} x_1 & x_{1+J} & x_{1+2J} & \dots & x_{1+(m-1)J} \\ x_2 & x_{2+J} & x_{2+2J} & \dots & x_{2+(m-1)J} \\ x_3 & x_{3+J} & x_{3+2J} & \dots & x_{3+(m-1)J} \\ \vdots & \vdots & \vdots & \ddots & \vdots \\ x_M & x_{M+J} & x_{M+2J} & \dots & x_{M+(m-1)J} \end{bmatrix} \quad (1)$$

where  $J$  is the lag time or reconstruction delay,  $m$  is the embedding dimension and  $M$  is the number of vectors reconstructed from the original time series. Thus the dimension of  $\mathbf{X}$  is an  $M \times m$  matrix.

Lyapunov exponent algorithm is an old methodology and has been reported in some areas such as the biomedical engineering field, especially to analyse electroencephalography (EEG) signals (Päivinen, et al 2005). As mentioned earlier, the LLE algorithm measures the exponential divergence (positive or negative) of two initial neighbouring trajectories in a phase space. The objective is to quantify the appearance of disturbances corresponding to signal abnormality. In other words, LLE algorithm measures the degree of chaos in certain time due to any disturbances. In this paper the term disturbances refers to any local instability vibration signal due to the dynamical contact between rolling elements and defect spots. This paper uses the LLE algorithm proposed by (Rosenstein, et al 1993). This algorithm is suitable for small data sets, as required in this work.

### 3. Circular Features Analysis

Circular feature analysis is a sub-area of statistics which allows computing the statistic properties such as mean, skewness and kurtosis of data distributed in a circular or angular domain, unlike from general statistical analysis which calculates

the features from data distributed in the time domain. In this paper, circular features calculation is used to analyse the data obtained from LLE algorithm. As mentioned earlier, LLE is employed to identify the stable or chaotic condition of raw vibration data in discrete angular positions ( $6^\circ \approx 1$  s). The illustration application of LLE algorithm as chaos detection method and circular analysis is presented in Picture 2, which is based on the laboratory data obtained as described in Section 4. A set of 30 seconds raw vibration data is used as the input to the LLE algorithm, where every 1 second data ( $\approx 4880$  data points) is analysed to identify whether the data represents a stable or chaotic condition. In the Picture, the "star" signs represent stable conditions (negative  $\lambda_1$ ) while the "cross" signs represent chaotic condition (positive  $\lambda_1$ ). In Picture 2 all data are transformed into the circular or angular domain, but in the Picture 5 only the stable condition is transformed in order to do the circular-domain features extraction. It noted that the stable condition will occur less and less frequently as the fault progresses.

The vibration data used for illustration in Picture 2 is the raw vibration data collected experimentally on March 26<sup>th</sup>. In order to calculate the circular features, the particular time when the stable condition (negative  $\lambda_1$ ) occurred is recorded. Then, it is transformed in the angular domain by the following expression:

$$\alpha = \left( \frac{t}{t_{\max}} \right) \cdot \left( \frac{\beta}{360} \right) \cdot 2\pi \quad (2)$$

where  $t$  is the time of recorded negative sign,  $t_{\max}$  is the time when the slewing bearing rotates ( $t_{\max} = 30$  s) and  $\beta$  is the reversible angle of the slewing bearing ( $\beta=180^\circ$ ). The result of the negative  $\lambda_1$  distributed in circular or angular domain as shown in Picture 5(a) and 5(b).

#### Circular mean and mean resultant vector:

The mean of vector  $\alpha$  cannot be estimated using simple linear averaging data points. Since  $\alpha$  is in angular directions, it is transformed into unit vectors in a two-dimensional plane by

$$Z_i = r \cos \alpha_i \text{ or } Z_i = r \sin \alpha_i \quad (3)$$

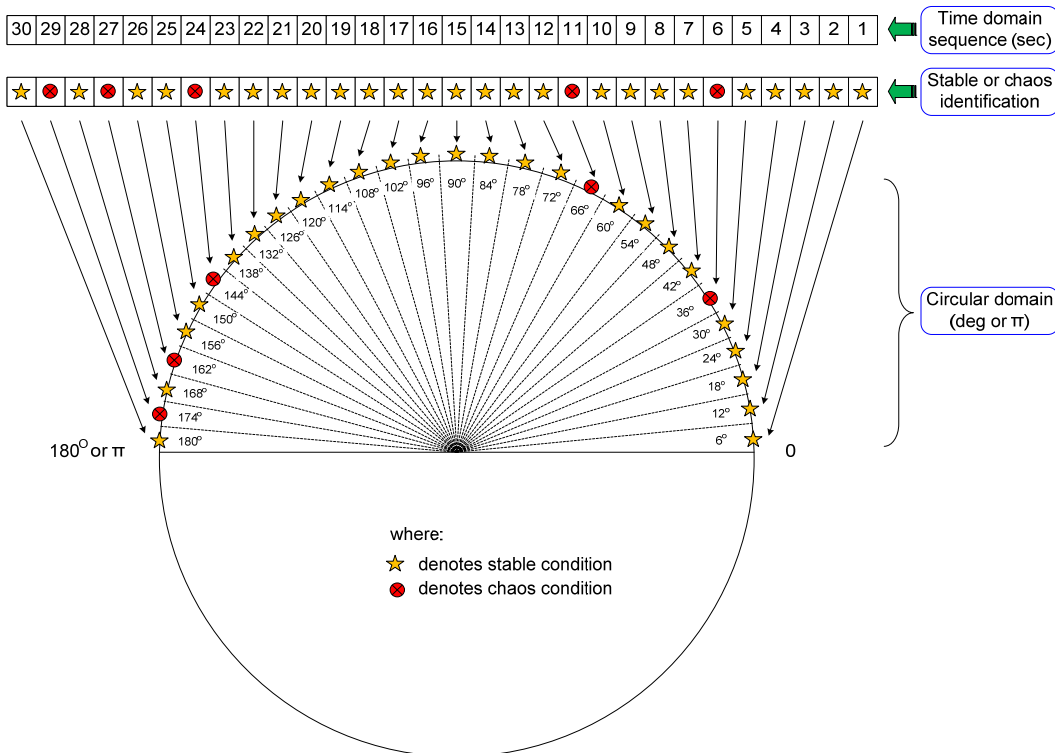
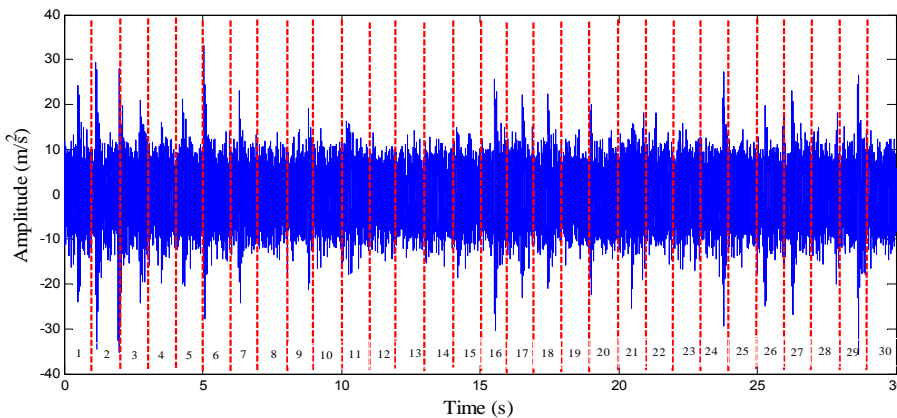
where  $r$  is the radius of the two-dimensional circular plane ( $r = 1$  is used in this paper). After this transformation, the mean of  $\bar{Z}$  can be computed from the vectors  $Z_i$  by

$$\bar{Z} = \frac{1}{C} \sum_i Z_i \quad (4)$$

where  $C$  is the number of data points (of positive sign). The vector  $\bar{Z}$  is the mean resultant vector. We have used the built-in function “angle” in MATLAB to calculate the circular mean by transforming  $\bar{Z}$  into the circular mean  $\bar{\alpha}$ . Further,  $i$  indicates the points in the circular domain where the positive signs indicating the chaos occur. The

length of the mean resultant vector is an important quantity for the measurement of circular spread<sup>(13)</sup> in the circular domain (Berens, 2009), the more concentrated the data sample is around the mean direction. The resultant vector length is estimated by

$$R = \|\bar{Z}\| \quad (5)$$



Picture 2 Time-domain to circular-domain transformation for stable or chaos condition identification (this illustration is constructed based on the vibration data of March 26<sup>th</sup> 2007)

**Circular skewness:**

As the third order statistical moments, circular skewness quantifies the symmetry of distribution data with respect to the circular mean. In circular domain, we used the circular skewness formula proposed by (Fisher, 1995):

$$s = \frac{R_2 \sin(\bar{\alpha}_2 - 2\bar{\alpha})}{(1 - R)^{2/3}} \quad (6)$$

**Circular kurtosis:**

Similar to time-domain kurtosis feature, circular kurtosis measures the degree of the scatter of the distribution around the peak. Kurtosis reflects the condition of the bearing and provides potential damage detections at an earlier stage. In case of linear scale kurtosis, when the rolling elements roll across the defects spot, it produces responsive signal that has probability density sharper than a normal condition (Caesarendra, et al 2010). We also used Fisher’s formula (Fisher, 1995) to compute circular kurtosis as defined

$$k = \frac{R_2 \cos(\bar{\alpha}_2 - 2\bar{\alpha}) - R^4}{(1 - R)^2} \quad (7)$$

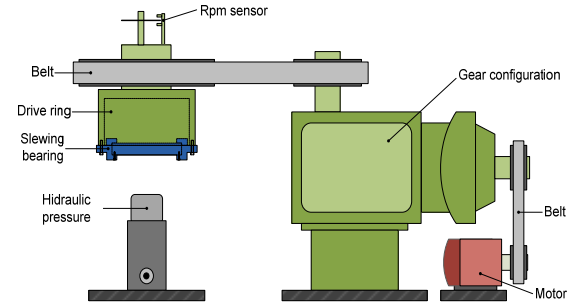
This formula assumes that the angular data  $\alpha_i$  follow a von Mises distribution, which is the circular analogue of the Normal distribution,  $k = 0$  (Berens, 2009), where  $R_2$  and  $\bar{\alpha}_2$  are obtained from the decomposition of the centered trigonometric moments,  $m_2$ , defined as the moments relative to the sample mean (Berens, 2009):

$$m_2 = \frac{1}{C} \sum_{i=1}^C \cos 2(\alpha_i - \bar{\alpha}) + i \frac{1}{C} \sum_{i=1}^C \sin 2(\alpha_i - \bar{\alpha}) \quad (8)$$

**4. Experimental setup**

The vibration data used in this paper was acquired from a laboratory slewing bearing test-rig. The test-rig can be operated at speeds of 1 to 12 rpm. The test-rig was designed to simulate the real working conditions of a steel making company. In this paper, the test-rig was operated in reversible rotation at speed of 1 rpm. The slewing bearing used was an axial/radial bearing supplied by Schaeffler (INA YRT260) with inner and outer diameters of 260mm and 385mm, respectively. The vibration data were acquired from four accelerometers installed on the inner radial surface at 90 degree to each other. The accelerometers were of the IMI608 A11 type.

They were connected to high speed Pico scope DAQ (PS3424). The data was collected daily with 4880Hz sampling rates during a 138-day period from February to August 2007. Each day the data were acquired for approx. 2 minutes. In order to accelerate the bearing defect, coal dust was injected into the bearing on April 2007. The schematic diagram of the laboratory slewing bearing test-rig is shown in Picture 3. The fault slewing frequencies are presented in Table 1.



Picture 3 Schematic of Laboratory slewing bearing test-rig

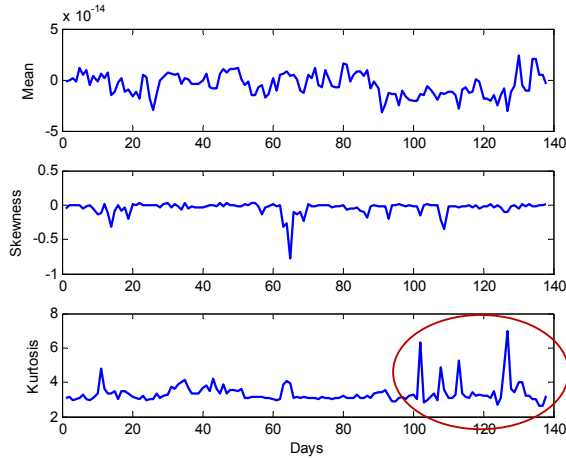
Defect mode	Axial	Radial
BPFI (Hz)	1.32	0.55
BPFO (Hz)	1.37	0.55
BSF (Hz)	0.43	0.54

Table 1 Fault frequencies of slewing bearing (calculated from appendix A)

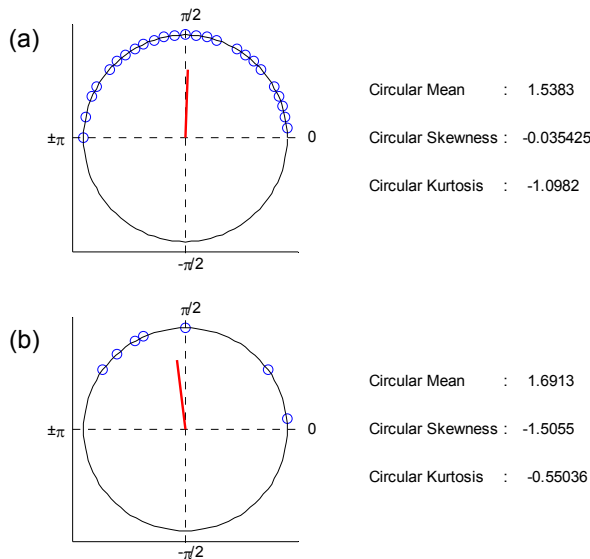
**5. Results and discussion**

In common vibration analysis, the appearance of faults can normally be identified when fault frequencies emerge (Siegel, et al 2012). FFT has been used for this purpose but the slewing bearing fault frequencies, presented in Table 1, are difficult to identify. The vibration signal is dominated by the high frequency components which mask the low-energy and low-frequency of slewing bearing. Then, the time-domain features such as mean, skewness and kurtosis are calculated from February to August 2007 (138 days). The results of the feature extractions are presented in Picture 4. It can be seen that the alteration of bearing condition from normal to failure (February to August 2007) are not obvious from mean and skewness features; only kurtosis, in contrast to mean and skewness, shows fluctuations in the end of the bearing running time. Based on the kurtosis feature calculation result, we assumed that there is performance

deterioration in the last period, namely during August 2007. We also calculated other time-domain features such as entropy, upper and lower histogram based on (Widodo, et al 2007). For brevity, the results are not shown here; however, they do not indicate any deterioration similar to mean and skewness.



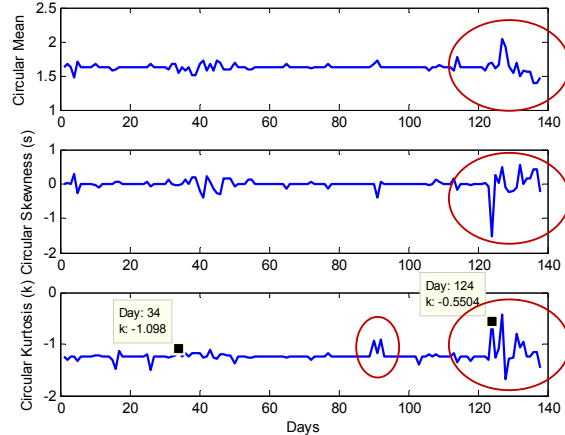
Picture 4 Linear time-domain features extraction



Picture 5 Example of positive sign occurrence (chaos) in circular domain plot and circular feature extraction on (a) March 26<sup>th</sup> 2007 (day 34<sup>th</sup>); (b) August 17<sup>th</sup> 2007 (day 124<sup>th</sup>)

We, then, applied LLE algorithm to assess the condition of slewing bearing in each second ( $\approx 6^\circ$ ) of vibration signal, containing 4880 data points. As mentioned in Section 2, the LLE algorithm measures the exponential divergence (positive or

negative) of two initial neighbouring trajectories in a phase space. According to Eq. (9) negative  $\lambda_1$  means the bearing signal (4880 data points) is stable and positive  $\lambda_1$  means the bearing signal is chaotic.



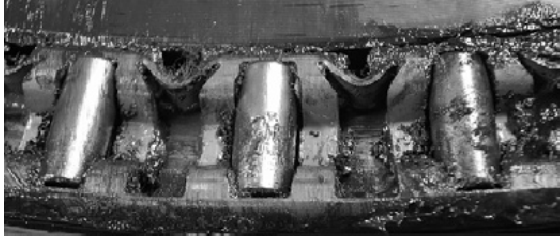
Picture 6 Circular features extraction result based on circular analysis and LLE algorithm

In the circular analysis method, the stable condition is recorded and the chaos condition is discarded. The time (second) when the stable condition recorded is transformed into the circular-domain. It can be seen from Picture 5(a) and (b) that the stable condition is distributed or lies in the angular or circular domain marked by the circle. As can be seen, in the beginning of the bearing running condition, i.e. March 26<sup>th</sup>, most of the circle line lies on the angular scale shown in Picture 5(a). As time progresses, the portion of the large circle occupied by small circle markers decrease as shown in Picture 5(b). This indicates that chaotic conditions occur more frequently than stable conditions during 30 second of raw vibration data. Further statistical tools are needed to compute the difference accurately. Hence, the circular features calculation such as circular mean, circular skewness and circular kurtosis proposed by (Fisher, 1995) are employed. The one day result of these three circular features are shown in the right side of Picture 5(a) and Picture 5(b). By computing the circular mean, circular skewness and circular kurtosis daily from February to August (138 days), we have the bearing performance deterioration condition shown in Picture 6.

As can be seen from Picture 6, the three circular features show consistent results, with fluctuations in the last period of the bearing running time



(approx. 120-138 days). This condition is similar to that detected by the linear time-domain kurtosis of Picture 4 (bottom) where the fluctuations occur at approx. 100-130 days. To confirm the result, the slewing bearing was dismantled for inspection after August 31<sup>st</sup> 2007, i.e. after day 138. The deteriorated regions found can be clearly seen in Picture 7.



Picture 7 (a) A view of damaged rollers in axial plane (b) Outer raceway damage

## 6. Conclusions

Feature extraction results of combined LLE algorithm and circular-domain features presented more sensitive than time-domain features in monitoring the bearing condition. It is pointed out that the effectiveness of circular-domain features extraction based on circular analysis and LLE algorithm is the consistency results of mean, skewness and kurtosis feature in which the features are more fluctuated when the bearing has been rotating about 123 days (August 2007). On the contrary the only sensitive feature in time-domain features is kurtosis. Another merit is the short dynamical changes due to dust inserted (approx. 40 days from the beginning) and the incipient fault (90 days from the beginning) can be identified. However, the proposed method has shortcoming that is the calculation time of proposed method take longer than time-domain features extraction. It is because of the LLE algorithms works based on phase space vector with predetermined lag time and embedding dimension.

In conclusion, the sensitive features that represent the bearing condition are needed in order to estimate the degradation index for prognosis method.

## 7. Acknowledgements

The first author acknowledges the University of Wollongong financial support through University Postgraduate Award (UPA) and International Postgraduate Tuition Award (IPTA).

## 8. Appendix A: Slewing bearing fault frequencies (Eschmann, et al 1953)

- Fault frequency of outer ring (BPFO):

$$F_{OR} = \left| \frac{IR_{rpm} - OR_{rpm}}{2} \right| \cdot \left[ 1 - \frac{(\cos(\alpha)) \cdot d_r}{d_m} \right] \cdot z \quad (A1)$$

- Fault frequency of inner ring (BPFI):

$$F_{IR} = \left| \frac{IR_{rpm} - OR_{rpm}}{2} \right| \cdot \left[ 1 + \frac{(\cos(\alpha)) \cdot d_r}{d_m} \right] \cdot z \quad (A2)$$

- Fault frequency of rolling element (BSF):

$$F_R = \left| \frac{IR_{rpm} - OR_{rpm}}{2} \right| \cdot \left[ \frac{d_m}{d_r} - \frac{(\cos(\alpha))^2 \cdot d_r}{d_m} \right] \quad (A3)$$

Where  $IR_{rpm}$  and  $OR_{rpm}$  are the rotational speed of the inner ring and outer ring respectively. For 1 rpm the value of  $IR_{rpm}$  is 1 and the value of  $OR_{rpm}$  is 0.  $d_m$  denotes the mean bearing diameter,  $d_r$  is diameter of the rolling element and  $z$  is number of rolling elements.

## 9. References

- Tan, A. C. C., Kim, Y.-H. and Kosse, V. (2008). Condition monitoring of low-speed bearing – a review, Australian Journal of Mechanical Engineering, Vol. 6, no.1, pp. 61-68.
- Kania, L. (2006). Modeling of rollers in calculation of slewing bearing with the use of finite elements, Mechanism and Machine Theory, Vol. 41, no.11, pp. 1359-1376.

- Göncz, P., Potočnik, R. and Glodež, S. (2011). Load capacity of a three-row roller slewing bearing raceway, *Procedia Engineering*, Vol. 10, pp. 1196-1201.
- Gang, Z., Xue, Z., Kaifeng, Z., Juan, R., Dede, J., Qingzhen, Y., Mingyan, L. and Yan, Z. (2011). Optimization design of large-scale cross-roller slewing bearing used in special propeller, *Applied Mechanics and Materials*, Vol. 48-49, no.2 pp. 787-792.
- Glodež, S., Potočnik, R. and Flašker, J. (2012). Computational model for calculation of static capacity and lifetime of large slewing bearing's raceway, *Mechanism and Machine Theory*, Vol. 47, pp. 16-30.
- Aguirrebeitia, J., Abasolo, M., Avilés, R. and Fernández de Bustos, I. (2012). Theoretical calculation of general static load-carrying capacity for the design and selection of three row roller slewing bearings, *Mechanism and Machine Theory*, Vol. 48, pp. 52-61.
- Bai, X., Xiao, H. and Zhang, L. (2011). The condition monitoring of large slewing bearing based on oil analysis method, *Key Engineering Materials*, Vol. 474-476, pp. 716-719.
- Liu, R. (2007). Condition monitoring of low-speed and heavily loaded rolling element bearing, *Industrial Lubrication and Tribology*, Vol. 59, no.6, pp.297-300.
- Rodger, L. M. (1979). The application of vibration signature analysis and acoustic emission source location to on-line condition monitoring of anti-friction bearings, *Tribology International*, Vol. April, pp. 51-59.
- Žvokelj, M., Zupan, S. and Prebil, I. (2010). Multivariate and multiscale monitoring of large-size low-speed bearings using ensemble empirical mode decomposition method combined with principal component analysis, *Mechanical Systems and Signal Processing*, Vol. 24, no.4, pp. 1049-1067.
- Žvokelj, M., Zupan, S. and Prebil, I. (2011). Non-linear multivariate and multiscale monitoring and signal denoising strategy using kernel principal component analysis combined with ensemble empirical mode decomposition method, *Mechanical Systems and Signal Processing*, Vol. 25, no.7, pp. 2631-2653.
- Päivinen, N., Lammi, S., Pitkänen, A., Nissinen, J., Penttonen, M. and Grönfors, T. (2005). Epileptic seizure detection: A nonlinear viewpoint, *Computer methods and Programs in Biomedicine*, Vol. 79, no.2, pp. 151-159.
- Berens, P. (2009). CircStat: A MATLAB toolbox for circular statistics, *Journal of Statistical Software*, Vol. 31, no.10, pp. 1-21.
- Fisher, N. I. (1995). *Statistical analysis of circular data*, Revised edition, Cambridge University Press.
- Pewsey A. (2004). The large-sample joint distribution of key circular statistics, *Metrika*, Vol. 60, no.1, pp. 25-32.
- Rosenstein, M.T., Collins J.J., De Luca C.J. (1993). A practical method for calculating largest Lyapunov exponents from small data sets, *Physica D*, Vol. 65, pp. 117-134.
- Caesarendra W., Widodo A. and Yang B. S. (2010). Application of relevance vector machine and logistic regression for machine degradation assessment, *Mechanical Systems and Signal Processing*, Vol. 24, no.4, pp. 1161-1171.
- Eschmann P., Hasbargen L. and Weigand K. (1953). *Die Wälzlagerpraxis: Handbuch für die Berechnung und Gestaltung von Lagerungen*, Publisher: R. Oldenburg.
- Siegel, D., Al-Atat, H., Shauche, V., Liao, L., Snyder, J. and Lee, J. (2012). Novel method for rolling element bearing health assessment – A tachometer-less synchronously average envelope feature extraction technique, *Mechanical Systems and Signal Processing*, Vol. 29, pp. 362-376.
- Widodo A. and Yang, B. S. (2007). Application of nonlinear feature extraction and support vector machines for fault diagnosis of induction motors, *Expert Systems with Applications*, Vol. 33, no.1, pp. 241-250.